

## Temperature dependence of the magnetoresistance of $\text{In}_x\text{Ga}_{1-x}\text{As}$ antidot lattices

J. Heremans, B. K. Fuller, and C. M. Thrush

*General Motors Research and Development Center, 30500 Mound Road, Warren, Michigan 48090*

V. Bayot

*Unité de Physico-Chimie et Physique des Matériaux, Université Catholique de Louvain,*

*Place Croix du Sud 1, B-1348 Louvain-la-Neuve, Belgium*

(Received 8 August 1995)

The magnetoresistance of two samples with antidot lattices fabricated in a two-dimensional electron gas in the lattice-matched  $\text{In}_{0.53}\text{Ga}_{0.47}\text{As}/\text{InP}$  system is studied as a function of temperature ( $3\text{ K} < T < 120\text{ K}$ ). Magnetoresistance peaks due to geometrical resonances are observed up to temperatures above 100 K. The purpose of this study is to provide experimental data on the dependence of the amplitude of the magnetoresistance peaks on temperature, along with mobility data in the same temperature range. The broadening of the peaks with increasing temperature is consistent with the thermal smearing of the Fermi surface. The reduction of the amplitude of the peaks is in part due to thermal smearing, but also to the increase in the electron-scattering rate. The temperature-dependent part of the electron-scattering time in antidot arrays is deduced from the amplitude reduction, and compared to the mobility relaxation time. [S0163-1829(96)05127-2]

### INTRODUCTION

The transport properties in two-dimensional electron systems (2DES's) patterned with a periodic array of antidots, regions in the 2DES's with a strongly repulsive potential, have been extensively studied since the beginning of the decade.<sup>1-4</sup> Reviews can be found in Refs. 5 and 6. In particular, the array of antidots can be configured following various arrangements: square,<sup>1-4</sup> triangular,<sup>7</sup> or hexagonal,<sup>8</sup> in a Penrose lattice,<sup>9</sup> and following various degrees of disorder.<sup>10-12</sup>

The magnetoresistance of an antidot lattice shows a maximum when the classical cyclotron orbit is commensurate with its lattice spacing. The size of the antidots and their lattice constant are usually smaller than the electron mean free path, and larger than the Fermi wavelength. The magnetoresistance peaks have been explained by the *ad hoc* assumption of pinned classical cyclotron orbits,<sup>1</sup> classical analytic expressions were published,<sup>13</sup> and a pinning mechanism was given.<sup>14</sup> Most of the reported data have been obtained in the liquid-helium temperature range, because phonon scattering drastically limits the high-temperature mean free path in the (AlGa)As system, in which most of the work has been carried out. It has been observed that the magnetoresistance peaks in antidot systems have substantially less temperature dependence than the Shubnikov-de Haas (SdH) oscillations,<sup>15</sup> but no systematic study of this has been reported. The only other study of the temperature dependence of mesoscopic transport over the temperature range reported here concerns data on the amplitude of transverse focusing peaks in  $\text{In}_{0.53}\text{Ga}_{0.47}\text{As}$  on InP.<sup>16</sup>

The present work is a systematic study of the amplitude of the magnetoresistance peaks as a function of temperature. Its aim is to provide data over as wide a temperature range as possible, using a semiconductor system with narrower gap than GaAs, and less phonon scattering at high temperature: the 2D electron gas at the heterointerface in the lattice-

matched  $\text{In}_{0.53}\text{Ga}_{0.47}\text{As}/\text{InP}$  system. On the basis of an analysis of the temperature dependence of both the width and the amplitude of the magnetoresistance peaks, we suggest that that the measurements may be explained by the thermal smearing of the Fermi surface, combined with the temperature dependence of the electron-scattering time.

### EXPERIMENT

The lattice-matched  $\text{In}_{0.53}\text{Ga}_{0.47}\text{As}$  film on InP used in this study is grown by metal-organic chemical-vapor depositor (MOVCD), and has the following profile: InP substrate (Fe doped)/400-nm undoped InP/12-nm InP:Si,  $n = 1.0 \times 10^{18}\text{ cm}^{-3}$ /20-nm undoped InP spacer/100 nm  $\text{In}_x\text{Ga}_{1-x}\text{As}$ . The sample is the same as the one labeled R540 in Ref. 16, where the temperature dependence of its mobility is reported. The electron effective mass in  $\text{In}_{0.53}\text{Ga}_{0.47}\text{As}$  is  $m^* = 0.045m_e$ ,<sup>17</sup> where  $m_e$  is the free-electron mass. Two antidot samples are made from this film, one of which (sample A) is shown in Fig. 1: it is shaped as a mesa-etched rectangular Hall bar defined photolithographically, with two current contacts, and two sets of four voltage probes. The set at the left-hand side is used to measure the magnetoresistance and Hall voltage of the unpatterned area, while the contacts on the right measure the area into which antidots have been etched, using electron-beam lithography and wet chemical etching. The nominal geometrical dimensions of the antidots, obtained from scanning electron microscopy (SEM) micrographs, can be deduced from the bottom frame in Fig. 1. The antidots are rectangular in shape, due to the anisotropy of the wet etch and possibly to the astigmatism in the  $e$ -beam processing, with geometrical dimensions of  $120 \times 250\text{ nm}^2$  approximately. They are arranged in a rectangular lattice with a  $400 \times 450\text{-nm}^2$  periodicity. The second sample (B) has antidots of the same size, but they are arranged in a rectangular lattice with  $500 \times 600\text{-nm}^2$  periodicity, and thus there is more  $\text{In}_x\text{Ga}_{1-x}\text{As}$  material between antidots in sample B than in

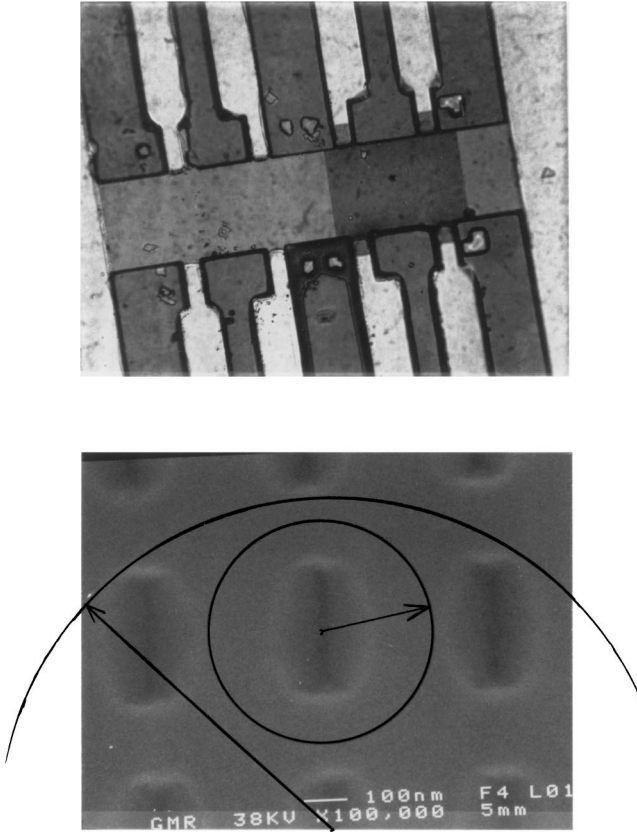


FIG. 1. The patterns on sample A: the optical micrograph (top: the device width is  $50\ \mu\text{m}$ ) shows the current contacts (left and right), and eight voltage contacts: four on the unpatterned area of the mesa, and four of the part of the film into which antidots have been etched. The electron micrograph (bottom) shows the antidots, which are rectangularly shaped. The smallest circle drawn has a radius of  $260\ \text{nm}$ , the larger of  $790\ \text{nm}$ .

sample A. The electrical widths of the regions between antidots can vary appreciably from the geometrical dimensions, because of the existence of a depletion layer around the mesa edge.

The antidot samples are measured in fields from  $-2\ \text{T} < H < 5\ \text{T}$  at temperatures from  $1.4$  to  $180\ \text{K}$ . The region of the Hall bar without antidots is used to analyze the low-field Hall density and mobility. Below  $30\ \text{K}$ , it is also possible to analyze the SdH oscillations both on the pristine and on the antidotted region. On sample B, Fourier analyses of the SdH oscillations give an electron density  $N_a = 4.8 \times 10^{11}\ \text{cm}^{-2}$  in the region without antidots, and  $5.3 \times 10^{11}\ \text{cm}^{-2}$  in the region with antidots, while low-field Hall data on the pristine region at the same temperature ( $4.3\ \text{K}$ ) give  $6.0 \times 10^{11}\ \text{cm}^{-2}$  during the same cooldown. On sample A, the density at  $4.2\ \text{K}$  is about 10% higher. In all cases, only one sublevel is occupied. The residual mobilities below  $10\ \text{K}$ , obtained from the low-field Hall measurements, are  $135\ 000\ \text{cm}^2/\text{Vs}$  for sample A and  $123\ 000\ \text{cm}^2/\text{Vs}$  for sample B. The electron densities are weakly temperature dependent (a Hall density of  $7.7 \times 10^{11}\ \text{cm}^{-2}$  is measured at  $100\ \text{K}$  on sample B). The Hall densities vary by 20–30% from cooldown to cooldown, while the mobilities remain within 3–4%; the values reported above are those obtained during the cooldown, during which all the other data reported in this paper are measured.

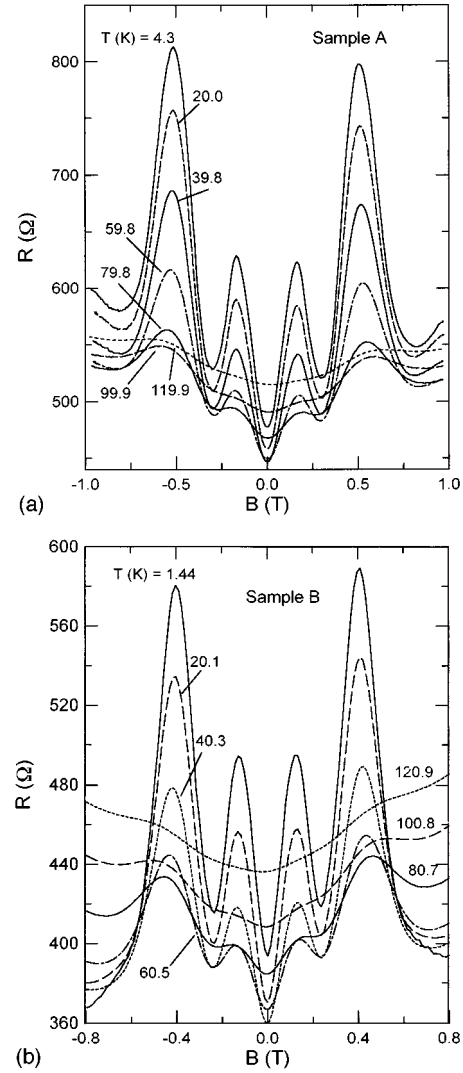


FIG. 2. Field dependence of the magnetoresistances of the regions with antidots of sample A (top, antidots pattern in a  $400 \times 450\text{-nm}^2$  lattice) and of sample B (bottom, antidot pattern in a  $500 \times 600\text{-nm}^2$  lattice), at various temperatures.

From the areal density  $N_a$  and the mobility  $\mu$ , the mobility mean free path  $l_\mu$  can be calculated:

$$l_\mu = (\hbar/e)\mu(2\pi N_a)^{1/2}. \quad (1)$$

This varies in both samples from approximately  $1600\ \text{nm}$  at  $4.2\ \text{K}$  to approximately  $700\ \text{nm}$  at  $100\ \text{K}$ , and is larger than the perimeter of the cyclotron orbit pinned around a single antidot, but not larger than the orbit encompassing multiple antidots. From  $N_a$ , we can calculate the size of the Fermi wavelength, ( $30\ \text{nm}$ ), and verify that it is smaller than the geometrical dimensions.

The magnetoresistances and Hall resistances are measured using a standard dc technique, with currents of  $100\ \text{nA}$  to  $10\ \mu\text{A}$ ; the current intensity did not affect the data over this range. Each data point is the difference between the voltage values read with the current in both positive and negative polarities. Experimental curves for the magnetoresistance of the regions with antidots are shown in Fig. 2 for both samples A and B at various temperatures. The unpatterned part of each sample has a simple quadratic magnetoresis-

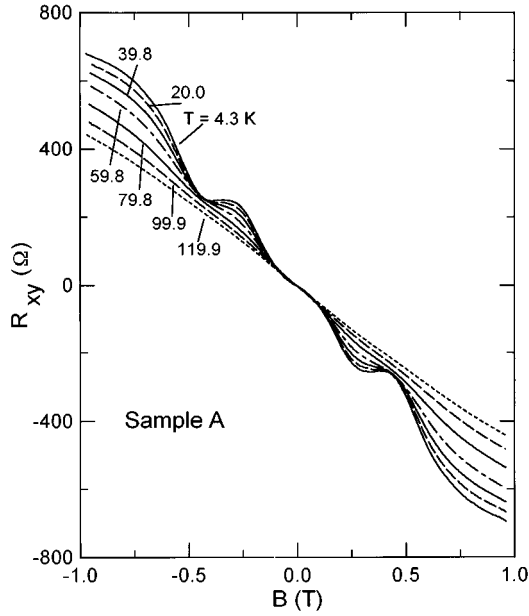


FIG. 3. Field dependence of the Hall resistance of the region of sample A with antidots.

tance, and linear Hall resistance for  $B < 0.4$  T with a slightly decreasing slope above 1 T. The departure from linearity of  $R_{xy}$ , and the quadratic magnetoresistance, are likely geometrical<sup>18</sup> effects, due to the rather square geometry seen in Fig. 1. The maxima in magnetoresistance occur at fields of  $B_m = \pm 0.514$  and  $\pm 0.169$  T for sample A, and  $\pm 0.408$  and  $\pm 0.132$  T for sample B. The cyclotron radii  $R_c$  are given semiclassically by<sup>6</sup>

$$B_m R_c = (\hbar/e) k_F = (\hbar/e) (2\pi N_a)^{1/2}. \quad (2)$$

The observed maxima correspond to radii of 260 and 790 nm for sample A, which are shown superimposed onto the SEM picture of the antidots in Fig. 1. The radii are 300 and 930 nm for sample B. The correspondence of the first-order peak confirms that we have reproduced on  $\text{In}_{0.53}\text{Ga}_{0.47}\text{As}$  the results that previous authors<sup>1-12</sup> obtained on GaAs at low temperature.

The Hall resistance  $R_{xy}$  (the transverse Hall voltage divided by the current) measured on the region with antidots of sample B is shown in Fig. 3; that of sample A has essentially the same shape and is therefore not reported. The steps in  $R_{xy}$  span the field range between the peaks in magnetoresistance in a manner consistent with the results reported on the (AlGa)As system.<sup>1,6</sup> A quenching of  $R_{xy}$  below 0.05 T is observed at the lowest temperatures, consistently with Ref. 6 though the sign of  $R_{xy}$  never reverses in our samples, presumably because their low-temperature mobility is 5–10 times smaller than the (AlGa)As samples of Ref. 6.

The magnetoresistance of sample B is also measured as a function of carrier density  $N_a$ . The electron density in this sample is systematically increased at 4.2 K by persistent photoconductivity. In this series of measurements, an  $\text{Al}_x\text{Ga}_{1-x}\text{As}$  light-emitting diode (LED) shines incremental amounts of photons on the sample, after which the complete magnetoresistance curve is measured. The electron Fermi en-

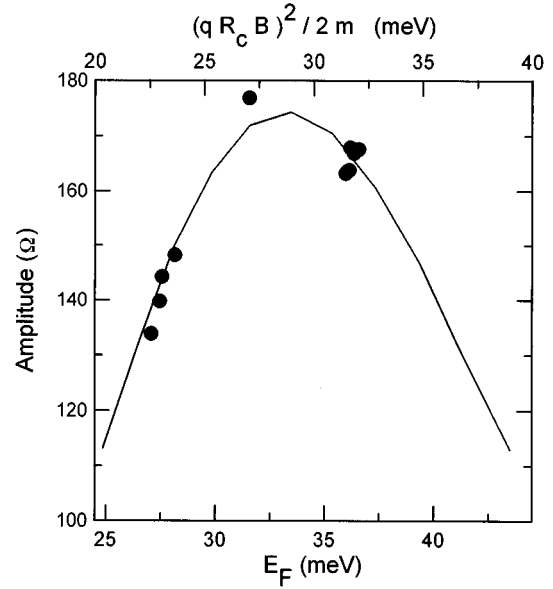


FIG. 4. The amplitude of the magnetoresistance peaks at a fixed field  $B = 0.429$  T plotted as a function of the Fermi energy in sample B (bottom abscissa, data points), which was varied by using persistent photoconductivity in the sample. The full line is the amplitude of the peak measured on sample B before illumination, plotted as a function of the quantity shown in the top abscissa. The data are taken at 4.3 K.

ergy for each trace is calculated using the densities obtained from the high-field SdH oscillations.

## RESULTS

The magnetoresistance data exhibit two peaks; a high-field one which corresponds to electrons orbiting around a single antidot, and a low-field one, which corresponds to electrons orbiting around a group of nine antidots. We note that the perimeter of the latter orbit is larger than the mobility mean free path  $l_\mu$ . The two peaks have essentially the same temperature dependence. The low-field peak is weaker, and, at high temperature, more difficult to extract from the quadratic magnetoresistance background. For that reason, the emphasis of this work is on the high-field peak, which is centered at 0.514 T for sample A and 0.408 T for sample B. The peak shape in (in  $\Omega$ ) is obtained as a function of the field  $B$  by subtracting from each value of  $R(B)$  the value of the resistance linearly interpolated between the minima in  $R(B)$  at either side of the peak, for instance, at  $B \approx 0.2$  and 0.75 T for sample B. In a first step, we illustrate in Fig. 4 the correspondence between the peak measured as a function of field with that measured as a function of energy in the illumination experiment. The amplitude of the magnetoresistance measured as a function of  $B$  on the unilluminated sample is plotted as a full line as a function of the quantity

$$E = (qR_c B)^2 / 2m^* \quad (3)$$

in the top abscissa. The series of points in Fig. 4 is the amplitude at a fixed field,  $B = 0.429$  T (0.021 T above the maximum in the unilluminated sample), obtained on the illuminated samples, and plotted as a function of the Fermi

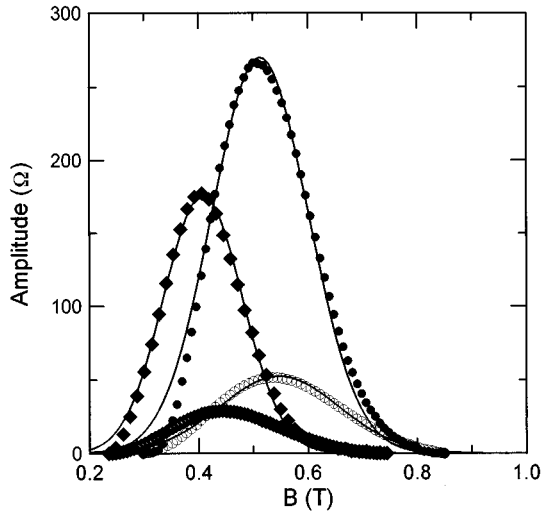


FIG. 5. The amplitude of the magnetoresistance peaks plotted as a function of magnetic field. The data points are ( $\blacklozenge$ , upper curve): sample A,  $T=4.2$  K; ( $\diamond$ , lower curve): sample A,  $T=79.8$  K; ( $\bullet$ ): sample B,  $T=4.2$  K; ( $\circ$ ), sample B,  $T=80.7$  K. The full lines are fits to Eq. (4).

energy (bottom abscissa). There is a shift of 4.5 meV between the top and the bottom abscissa, which corresponds exactly to the shift of 0.021 T. The agreement illustrates that Eq. (3) can be used to convert the peak shape from an energy axis to a field axis, and vice versa.

The shape of the magnetoresistance peak plotted as a function of field  $B$  is shown in Fig. 5. This shape depends<sup>14</sup> on the details of the chaotic trajectories of the electrons, and on the sharpness of the antidot potential. Nevertheless, in order to avoid having to use computer simulations to continue the analysis, we have fitted a Gaussian function

$$G(B) = (A/B_w)(4 \ln(2)/\pi)^{1/2} \exp[-4(B - B_c)^2/B_w^2]. \quad (4)$$

to the data, with an area  $A$ , a peak amplitude

$$A_p = (A/B_w)(4 \ln(2)/\pi)^{1/2} \quad (5)$$

at  $B = B_c$ , and a peak width  $B_w$ . The lines in Fig. 5 are fits to the peaks observed on both samples A and B at 4.2 K and 2.4 K and at 80 K. The fitted peak widths  $B_w$  are then plotted as a function of temperature in Fig. 6, and the amplitudes  $A_p$  are shown in Fig. 7. Sample B, in which there is more  $\text{In}_x\text{Ga}_{1-x}\text{As}$  between the antidots than in sample A, has a smaller peak width than sample A, but the same temperature dependence.

## DISCUSSION

Two factors enter the temperature dependence of the magnetoresistance peaks: the influence of the smearing of the Fermi surface, and the temperature dependence of the scattering time. The influence of these mechanisms on both peak width and peak amplitude is now discussed.

Starting with a discussion of the peak width, we note that sample A has a low-temperature width (0.25 T) that is broader than sample B (0.20 T), which may be related to the fact that there is more  $\text{In}_x\text{Ga}_{1-x}\text{As}$  material between the an-

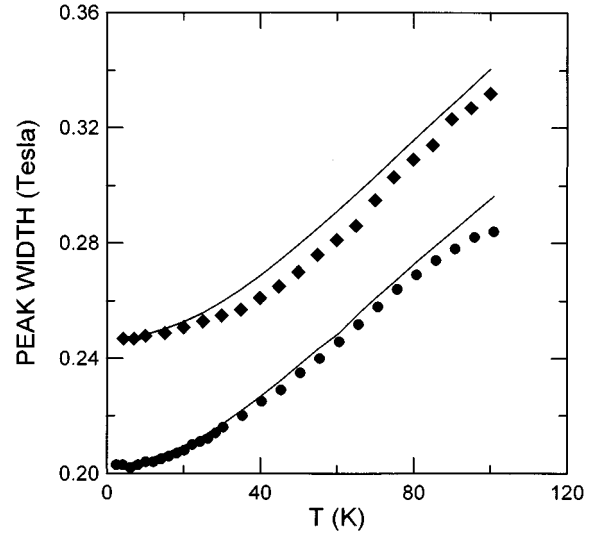


FIG. 6. The width of the peaks measured on samples A ( $\blacklozenge$ ) and B ( $\bullet$ ), plotted as a function of temperature. The lines are the widths of the peaks calculated from Eq. (6) for each sample.

tidots in sample B. On top of the low-temperature width comes a temperature-dependent part, which, when converted into Kelvin units using Eq. (3), corresponds to  $kT$ . To quantify this we combine the low-temperature Gaussian  $G(E)$ , obtained by transforming  $B$  into  $E$  using Eq. (3), with the derivative of the Fermi function  $df/dE$ , and write the temperature-dependent peak shape as

$$Am(T, B) = \left[ \int G(E) (-df/dE) dE \right] / N(T), \quad (6)$$

where  $N(T)$  is a normalization that keeps the integral under the peak a constant:

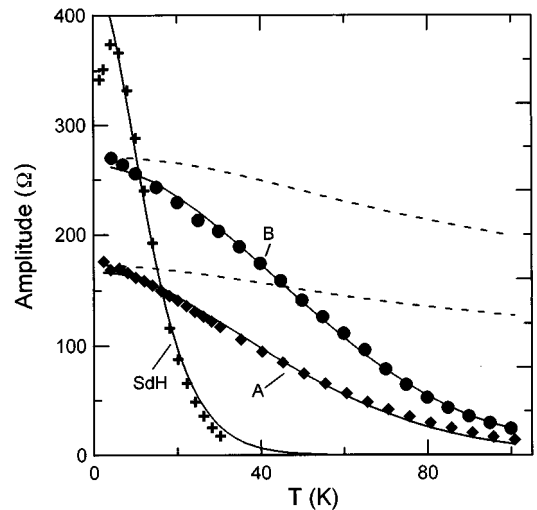


FIG. 7. The temperature dependence of the peak amplitude of samples A ( $\blacklozenge$ ) and B ( $\bullet$ ), as well as the amplitude of the Shubnikov–de Haas peak measured at 3.78 T on sample B ( $+$ ). The full lines are calculated by Eq. (8) for the SdH oscillations, and are fits to Eq. (8) for the magnetoresistance peaks labeled A and B. The dashed lines represent the peak amplitudes calculated from Eq. (6).

$$N(T) = \int Am(T, B) dB. \quad (7)$$

Both integrals are taken from zero to infinity. The widths of the peaks generated by Eq. (6) are plotted as a function of temperature in Fig. 6 as full lines, which reproduce the observed widths quite well.

We now turn to the temperature dependence of the peak amplitude: the dashed curves in Fig. 7 are the values of the amplitude that result from Eq. (6), and show much less decay with increasing temperature than the data points. Clearly there is a second mechanism at work: electron scattering.

The decrease of the amplitude of Shubnikov–de Haas oscillations with increasing temperature is described by the Dingle theory,<sup>19</sup> which uses the single-particle scattering time as opposed to the mobility relaxation time, and also describes the effect of Fermi smearing. The physical origin of the attenuation lies in the smearing of the phase of the SdH oscillations when the electron energy levels are broadened. The reduction of the amplitude of a SdH oscillation is described by a function

$$[(aT/B)\sinh(aT/B)]^* \exp(-p\pi/\omega_c\tau_s), \quad (8)$$

where the factor containing the hyperbolic sine describes the effect of the thermal smearing of the Fermi surface, and the exponential factor describes the effect of the finite single-particle scattering time  $\tau_s$ . Parameter  $a$  is related to the effective mass  $m^*$  of the carrier via

$$a = 2\pi^2 p k m^* / (e\hbar), \quad (9)$$

where  $p$  is the index of the harmonic of the oscillation (in the first order,  $p=1$ ). Equation (8) is used to calculate the temperature dependence of the amplitude of the SdH oscillation measured on sample A at the fixed field of 3.728 T: the data points are given as (+) symbols in Fig. 7, and the calculation with  $p=1$ , with the mass reported in the literature<sup>17</sup> and with  $\tau_s = \infty$ , is the full line through the crosses. The good agreement between the data and the Dingle theory shows that phase smearing dominates the temperature dependence of the SdH oscillations, while electron scattering is much less important in the temperature range in which the SdH oscillations are resolved ( $T \lesssim 30$  K). We now show that the geometrical resonances behave differently.

In a previous study<sup>16</sup> on the temperature dependence of the focusing peak in transverse focusing devices made from the same  $\text{In}_x\text{Ga}_{1-x}\text{As}$  material system as used here, we fitted Eq. (8) to the data, because of the similarities between the SdH oscillations and focusing: in neither case is the integral under the peaks constant with temperature, and both cases use  $\tau_s$  instead of the mobility relaxation time  $\tau_\mu$ . Hackenbroich and von Oppen<sup>20</sup> also used a similar equation to calculate the temperature dependence of the additional quantum oscillations observed by Weiss *et al.*<sup>21</sup> in the low-temperature ( $T \approx 0.4$  K) regime of an antidot lattice, but which are not of the same nature as the maximum studied here. A fit of Eq. (8), with the exponential factor replaced by  $\exp(-b\pi/\mu B)$ , where  $b$  and  $a$  are fitting parameters, to the amplitude data in Fig. 7, gives, for sample A,  $a=0.0209$  and  $b=1.0$ , and, for sample B,  $a=0.0197$  and  $b=1.0$ . The full lines labeled A and B in Fig. 7 correspond to these fits. The values for  $a$  are very similar to those obtained on the focus-

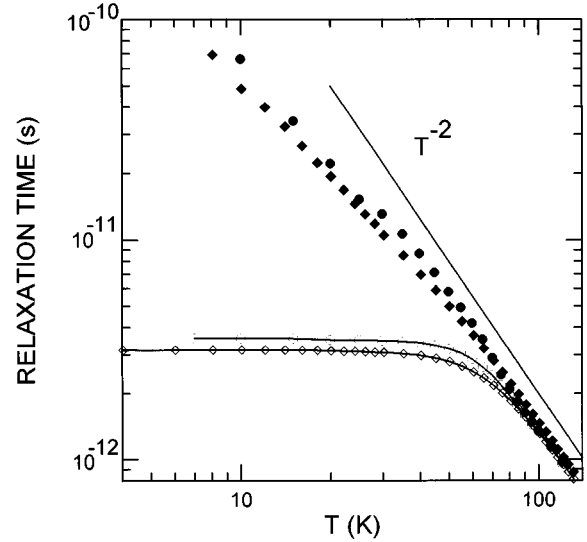


FIG. 8. The temperature-dependent fraction of the electron scattering time  $\tau_a$  in an antidot array (full symbols), and the mobility relaxation time  $\tau_\mu$  (open symbols) for samples A (diamonds) and B (circles and dots).

ing devices. Unfortunately, the masses that could be calculated from these values, and Eq. (9),  $0.00143m_e$  for sample A and  $0.00134m_e$  for sample B (assuming that  $p=1$ ), are 33 times smaller than observed on SdH oscillations. This is difficult to interpret, and simply parametrizes the observation that the antidot magnetoresistance peak decays more slowly with temperature than the SdH oscillations. Here we propose a different approach:<sup>22</sup> use the reduction in amplitude to calculate the temperature dependence of the electron scattering time  $\tau_a$  in antidot arrays, as a function of temperature.

Measurements of the amplitude of transverse electron focusing in metals<sup>23,24</sup> as well as in semiconductors<sup>25</sup> as a function of the distance the ballistic electrons have to travel show that the amplitude varies with the electron mean free path as

$$V/I = R_0 \exp[-(\pi/2)L_e/l_f], \quad (10)$$

where  $l_f$  is a characteristic focusing ballistic mean free path, and  $(\pi/2)L_e$  is the geometrical distance electrons travel in that structure. For each of the samples in Fig. 7, we fit the ratio of the data points to the dashed line which represents the Fermi smearing, Eq. (6), to a function equivalent to Eq. (10):

$$A_p = A_0 \exp(-2\pi/\omega_c\tau_a), \quad (11)$$

where  $\omega_c$  is calculated at the peak field. The factor  $2\pi$  assumes that an electron travels one single orbit around an antidot; this is clearly an approximation, since the orbits are chaotic. A visual representation of the pinned orbits is given in Fig. 8d of Ref. 6: their perimeter is somewhat larger than the perimeter of the inscribed circle, but not much. Therefore, while  $\tau_a$  is only known within a proportionality factor, that factor is not much larger than unity. The procedure gives only the temperature-dependent part of  $\tau_a$ , which is plotted in Fig. 8 along with that of the mobility relaxation time  $\tau_\mu = \mu q/m^*$  from the mobility data measured on the antidot-free part of each sample. The residual value of  $\tau_a$  is undeter-

mined, as it is incorporated into the prefactor  $A_0$ . Figure 8 shows that the temperature-dependent part of  $\tau_a$  follows roughly a  $T^{-2}$  law, and asymptotically joins  $\tau_\mu$  at higher temperatures.

One fundamental difference between  $\tau_\mu$  and  $\tau_a$  is the fact that the sensitivity of both to the angular dependence of the electron-scattering mechanism is different: in ballistic transport, small-angle scattering will also reduce the amplitude of the focusing peaks, or the antidot magnetoresistance peaks, while in diffusive transport each scattering event is attributed a weighing factor  $[1 - \cos(\theta)]$  where  $\theta$  is the scattering angle. Since  $\tau_a$  is expected to be more sensitive to the scattering angle than  $\tau_\mu$ , and the influence of small-angle scattering is expected to be more pronounced at lower temperatures where the dominant phonons have smaller momenta, the temperature dependence of  $\tau_a$  and  $\tau_\mu$  are expected to differ more at  $T < 60$  K. The agreement shown in Fig. 8 therefore illustrates that the temperature dependence of the peaks is well explained by Eq. (11).

### SUMMARY

Peaks have been observed in the magnetoresistance of the 2D electron gas at the interface between lattice-matched

$\text{In}_x\text{Ga}_{1-x}\text{As}$  on InP, modulated by square lattices of antidots, at temperatures in excess of 100 K, where electron-phonon interactions limit the mean free path. The width of the peaks increases with temperature in a way that is consistent with thermal broadening. The amplitude of the peaks decreases with increasing temperature through two mechanisms: the thermal smearing of the Fermi surface, and increased electron scattering. The data are used to determine the temperature dependence of the electron-scattering time in an antidot array. The quantitative agreement between that quantity and the mobility relaxation time at higher temperatures shows that the temperature dependence of the magnetoresistance is well described by the scattering time model.

### ACKNOWLEDGMENTS

The authors acknowledge useful conversations with Professor M. Shayegan, Professor W. Zawadzki, Dr. D. Weiss, Dr. G. L. Eesley, and Dr. J. J. Heremans, and Thaddeus Schroeder. V.B. acknowledges the financial support of the Belgian National Fund for Scientific Research.

- <sup>1</sup>D. Weiss, M. L. Roukes, A. Menshig, P. Grambow, K. von Klitzing, and G. Weimann, *Phys. Rev. Lett.* **66**, 2790 (1991).
- <sup>2</sup>A. Lorke, J. P. Kotthaus, and K. Ploog, *Phys. Rev. B* **44**, 3447 (1991); A. Lorke, *Surf. Sci.* **263**, 307 (1992).
- <sup>3</sup>K. Ensslin and P. M. Petroff, *Phys. Rev. B* **41**, 12 307 (1990).
- <sup>4</sup>G. M. Gusev, Z. D. Kvon, V. M. Kudryashov, L. V. Litvin, Yu. V. Nastaushev, V. T. Dolgopopov, and A. A. Shashkin, *Pisma Zh. Eksp. Teor. Fiz.* **54**, 369 (1991) [*JETP Lett.* **54**, 365 (1991)].
- <sup>5</sup>C. W. J. Beenakker and H. van Houten, in *Quantum Transport in Semiconductor Nanostructures*, edited by H. Ehrenreich and D. Turnbull, *Solid State Physics Vol. 44* (Academic, New York, 1991).
- <sup>6</sup>D. Weiss, K. Richter, E. Vasiliadou, and G. Lutjering, *Surf. Sci.* **305**, 408 (1994).
- <sup>7</sup>T. Tamashiro, J. Takahara, Y. Takagaki, K. Gamo, S. Namba, S. Takaoka, and K. Murase, *Solid State Commun.* **79**, 885 (1991).
- <sup>8</sup>J. Takahara, K. Gamo, S. Namba, S. Takaoka, and K. Murase, *Jpn. J. Appl. Phys.* **31**, 3786 (1992).
- <sup>9</sup>G. M. Gusev, P. Basmaji, D. I. Lubyshev, L. V. Litvin, Yu. V. Nastaushev, and V. V. Preobrazhenskii, *Phys. Rev. B* **47**, 9928 (1993).
- <sup>10</sup>G. M. Gusev, Z. D. Kvon, L. V. Litvin, Yu. V. Nastaushev, A. K. Kalagin and A. I. Toropov, *Pis'ma Zh. Eksp. Teor. Fiz.* **56**, 173 (1992) [*JETP Lett.* **56**, 170 (1992)].
- <sup>11</sup>G. M. Gusev, P. Basmaji, Z. D. Kvon, L. V. Litvin, Yu. V. Nastaushev, and A. I. Toropov, *J. Phys. Condens. Matter* **6**, 73 (1994).
- <sup>12</sup>G. M. Gusev, P. Basmaji, Z. D. Kvon, L. V. Litvin, Yu. V. Nastaushev, and A. I. Toropov, *Surf. Sci.* **305**, 443 (1993).
- <sup>13</sup>R. W. Tank and R. B. Stinchcombe, *J. Phys. Condens. Matter* **5**, 5623 (1993).
- <sup>14</sup>R. Fleischmann, T. Geisel, and R. Ketzmerick, *Phys. Rev. Lett.* **68**, 1367 (1992).
- <sup>15</sup>D. Weiss (private communication).
- <sup>16</sup>J. Heremans, B. K. Fuller, C. M. Thrush, and D. L. Partin, *Phys. Rev. B* **52**, 5767 (1995).
- <sup>17</sup>*Semiconductors, Physics of Group IV Elements and III-V Compounds*, edited by O. Madelung, M. Schulz, and H. Weiss, Landolt-Börnstein, New Series, Group III, Vol. 17, Part a (Springer-Verlag, Berlin, 1982).
- <sup>18</sup>J. Heremans, *J. Phys. D* **26**, 1149 (1993).
- <sup>19</sup>D. Schoenberg, *Magnetic Oscillations in Metals* (Cambridge University Press, Cambridge, 1984).
- <sup>20</sup>G. Hackenbroich and F. von Oppen, *Z. Phys.* **97**, 157 (1995) did derive that the temperature dependence of the conductivity tensor elements in an antidot lattice at very low temperature should be proportional to Eq. (9), where  $p$  counts the number of repeated traversals,  $\tau_s$  is now the elastic scattering time, and the length of the periodic orbit is  $L = 2\pi R_c$ , so that  $a = \pi p L k T / v_F \hbar = 2\pi^2 p k m^* / (e \hbar)$ .
- <sup>21</sup>D. Weiss, K. Richter, A. Menshig, R. Bergmann, H. Schweitzer, K. von Klitzing, and G. Weimann, *Phys. Rev. Lett.* **70**, 4118 (1993).
- <sup>22</sup>Suggested by M. Shayegan (private communication).
- <sup>23</sup>P. C. van Son, H. van Kempen, and P. Wyder, *Phys. Rev. Lett.* **58**, 1567 (1987).
- <sup>24</sup>P. A. M. Benistant, G. F. A. van de Walle, H. van Kempen, and P. Wyder, *Phys. Rev. B* **33**, 690 (1986).
- <sup>25</sup>J. Spector, H. L. Stormer, K. W. Baldwin, L. N. Pfeiffer, and K. W. West, *Surf. Sci.* **228**, 283 (1990).